

Article

# Synthesis of an Adduct-Type Organic Ionic Crystal with Solid-State Ionic Conductivity from A Thiocyanate-Based Ionic Liquid and $B(C_6F_5)_3$

Yui Oki <sup>1</sup> and Makoto Moriya <sup>1,2,\*</sup> 

<sup>1</sup> Department of Optoelectronics and Nanostructure Science, Graduate School of Science and Technology, Shizuoka University, 836 Ohya, Suruga-ku, Shizuoka 422-8529, Japan; oki.yui.16@shizuoka.ac.jp

<sup>2</sup> Academic Institute, College of Science, Shizuoka University, 836 Ohya, Suruga-ku, Shizuoka 422-8529, Japan

\* Correspondence: moriya.makoto@shizuoka.ac.jp; Tel.: +81-54-238-4753

Received: 29 September 2019; Accepted: 28 October 2019; Published: 29 October 2019



**Abstract:** We synthesized the novel adduct-type organic ionic crystal  $[C3mim][SCN \cdot B(C_6F_5)_3]$  (**1**) by the reaction of 1-methyl-3-propylimidazolium thiocyanate ( $[C3mim][SCN]$ ), which is a room temperature ionic liquid, and  $B(C_6F_5)_3$ , a bulky Lewis acid. The formation of a coordinative B–N bond between the SCN anion and the  $B(C_6F_5)_3$  in **1** was revealed by single-crystal X-ray diffractometry. We showed that **1** displays ionic conductivity in the crystalline state and that doping **1** with sodium thiocyanate and  $B(C_6F_5)_3$  results in a dramatic increase in ionic conductivity compared to that of **1**.

**Keywords:** organic ionic crystal; solid-state ionic conductivity; thiocyanate

## 1. Introduction

Ionic liquid crystals (ILCs) [1–3] and organic ionic plastic crystals (OIPCs) [4–6] have attracted considerable attention as matrix materials for the development of innovative solid electrolytes. Both liquid crystals and plastic crystals are intermediate phases that lie between crystals and liquids; hence, ILCs and OIPCs undergo phase transitions to organic ionic crystals (OICs), as low-temperature phases, upon cooling in a similar manner to ionic liquids (ILs). Interestingly, studies into solid-state ion diffusion through OICs are quite limited despite the applications of ILCs and OIPCs as electrolyte materials being vigorously studied.

On the other hand, we have reported ionic conduction through lithium-based OICs composed of lithium salts with organic anions and small molecules [7–11]. We found the formation of an ordered arrangement of lithium ions has been reported to be a key factor for lithium-ion diffusion in the crystal lattices of these lithium-based OICs. These results suggest that OICs composed of similar component units to ILs also have potential as matrix materials. Furthermore, such OICs are expected to exhibit favorable solid–electrolyte features, namely flame retardancy, non-volatility, and a wide potential window, such as those shown by ILs.

In order to synthesize such ion-conductive OICs, anions that are steric bulky compared to the cation are desirable. For example, we reported the phase-transition behavior of OIPCs composed of tetraalkylammonium or pyrrolidinium cations and the cyclic perfluorosulfonylamide anion,  $[N(SO_2CF_2)_2CF_2]^-$  (CPFSA) [12,13]. In this study, we showed that CPFSA-based OIPCs exhibit considerably high melting points compared to those of the analogous OIPCs that contain bis(trifluoromethanesulfonyl)amide ( $[N(SO_2CF_3)_2]^-$ , TFSA) because of the bulkiness of CPFSA. Moreover, the use of a large counter anion in an OIC is also expected to provide void structures that enhance ion diffusion in the crystal lattice.

In order to synthesize such ion-conductive OICs, anions that are steric bulky compared to the cation are desirable. For example, we reported the phase-transition behavior of OIPCs

composed of tetraalkylammonium or pyrrolidinium cations and the cyclic perfluorosulfonylamide anion,  $[\text{N}(\text{SO}_2\text{CF}_2)_2\text{CF}_2]^-$  (CPFSA) [12,13]. In this study, we showed that CPFSA-based OIPCs exhibit considerably high melting points compared to those of the analogous OIPCs that contain bis(trifluoromethanesulfonyl)amide ( $[\text{N}(\text{SO}_2\text{CF}_3)_2]^-$ , TFSA) because of the bulkiness of CPFSA. Moreover, the use of a large counter anion in an OIC is also expected to provide void structures that enhance ion diffusion in the crystal lattice.

One of the most useful techniques for increasing the size of an anion involves the formation of coordinative interactions between the coordinating anion and a bulky Lewis acid [14–16]. Previously, such adduct-type anions were prepared by the addition of the bulky  $\text{B}(\text{C}_6\text{F}_5)_3$  Lewis acid to anions containing cyano groups [16]. With this in mind, we synthesized ion conductive OICs using the 1-methyl-3-propylimidazolium thiocyanate ( $[\text{C3mim}][\text{SCN}]$ ) IL and  $\text{B}(\text{C}_6\text{F}_5)_3$  (Figure 1). Herein, we report the synthesis and crystal structure of  $[\text{C3mim}][\text{SCN}\cdot\text{B}(\text{C}_6\text{F}_5)_3]$  (**1**), a novel adduct-type OIC that exhibits ionic conductivity in the crystalline state. We also fabricated a solid-state ion-conductive OIC-based solid electrolyte by doping **1** with  $\text{NaSCN}$  and  $\text{B}(\text{C}_6\text{F}_5)_3$ .

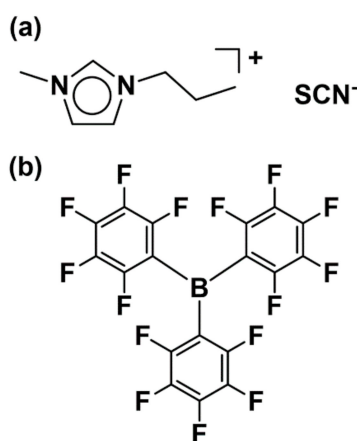


**Figure 1.** Molecular structures of the starting materials: (a)  $[\text{C3mim}][\text{SCN}]$  and (b)  $\text{B}(\text{C}_6\text{F}_5)_3$ .

## 2. Materials and Methods

All experiments were carried out under an argon atmosphere using Schlenk techniques or argon-filled glovebox (MBraun, UNIlab2000). Dehydrated THF, dehydrated pentane, and  $\text{NaSCN}$  were purchased from Kanto Chemical Co. (Tokyo, Japan) Tris(pentafluorophenyl) borane was purchased from Tokyo Chemical Industry Co. or gifted from Kanto Denka Kogyo Co., Ltd. (Tokyo, Japan)  $[\text{C3mim}][\text{SCN}]$  was prepared as reported [17]. The measurement of ion conductivity was performed using a disc of electrolyte sealed in a closed vessel. The disc was placed between two Au plates in a two-electrode cell. The temperature of cells was controlled by using a bench-top-type chamber (ESPEC, SU-241) and all cells were equilibrated at the operating temperature for at least 3 h before performing any measurements. Conductivity data were collected using a VMP3 (Biologic SAS, Seyssinet-Pariset, France) by AC impedance measurements over the frequency range between 1 Hz and 1MHz. Differential scanning calorimetry (DSC) analysis was performed by DSC60 instrument operated at a heating rate of  $10\text{ }^\circ\text{C min}^{-1}$  under a nitrogen atmosphere using  $\text{Al}_2\text{O}_3$  (Shimadzu Corporation, Kyoto, Japan) as reference material. Elemental analysis was performed on a Perkin Elmer 2400II CHNO/S elemental analyzer (Perkin Elmer Inc., MA, USA). Powder X-ray diffraction patterns were collected at room temperature with Rigaku Smart-Lab diffractometer ( $\text{CuK}\alpha$  radiation) (Rigaku Corporation, Tokyo, Japan).

**Synthesis of 1:**  $[\text{C3mim}][\text{SCN}]$  (0.4930 g, 2.69 mmol) was charged in a 50 mL reaction flask. Then,  $\text{B}(\text{C}_6\text{F}_5)_3$  (1.3810g, 2.70 mmol) dissolved in dehydrated THF was added to the flask. The reaction mixture was vigorously stirred at room temperature for 5 min to give a colorless homogeneous solution. Then, the solution was concentrated under reduced pressure. The obtained highly viscous liquid

crystallized gradually to give colorless single crystals at room temperature. The OIC **1** was obtained in 44% yield (0.815 g) by washing the crystals with dehydrated pentane followed by drying under reduced pressure at room temperature. Anal. calcd for  $C_{26}H_{13}BF_{15}N_3S$ : C, 44.92; H, 1.88; N, 6.04. Found: C, 44.77; H, 1.67; N, 5.49. Melting point: 99.8 °C.

**Fabrication of 1–0.1 and 1–0.2:** OIC **1** and 0.1 or 0.2 molar equivalents of NaSCN and  $B(C_6F_5)_3$  were charged in a 50 mL reaction flask. Then, the solid mixture was heated at 110 °C for 10 min to give colorless viscous liquid followed by cooling at room temperature to yield **1–0.1** or **1–0.2** as white solids.

**Crystallographic Structural Determination.** Data collections were carried out on a Rigaku VariMax Saturn (MoK $\alpha$  radiation, 1.2 kW rotating anode) (Rigaku Corporation, Tokyo, Japan). Crystal Data for  $C_{26}H_{13}BF_{15}N_3S$  (MW: 695.25): orthorhombic, Space Group  $P2_12_12_1$  (no. 19),  $a = 10.5887(12)$  Å,  $b = 13.1964(16)$  Å,  $c = 19.541(2)$  Å,  $V = 2730.5(5)$  Å<sup>3</sup>,  $Z = 4$ ,  $T = -120.0$  °C,  $\mu(\text{MoK}\alpha) = 2.454$  cm<sup>-1</sup>,  $D_{\text{calc}} = 1.691$  g/cm<sup>3</sup>, reflections collected/unique reflections/parameters refined: 31262/6244/417,  $R_{\text{int}} = 0.0173$ , final  $R_1 = 0.0317$  ( $I > 2\sigma(I)$ ),  $wR_2 = 0.0844$  (all data), GOF = 1.057. CCDC 1955625 contains the supplementary crystallographic data for this paper. These data can be obtained free of charge via <http://www.ccdc.cam.ac.uk/conts/retrieving.html> (or from the CCDC, 12 Union Road, Cambridge CB2 1EZ, UK; Fax: +44 1223 336033; E-mail: deposit@ccdc.cam.ac.uk).

### 3. Results and Discussion

Compound **1** was synthesized by the addition of [C3mim][SCN] to  $B(C_6F_5)_3 \cdot \text{THF}$  dissolved in dry THF under argon. The reaction proceeded at room temperature to give a colorless solution, which was evaporated under reduced pressure and cooled to give the **1** as colorless single crystals. [C3mim][SCN· $B(C_6F_5)_3$ ] (**1**) was subjected to differential scanning calorimetry (DSC), which revealed only one peak attributed to melting at 99.8 °C (Figure 2).

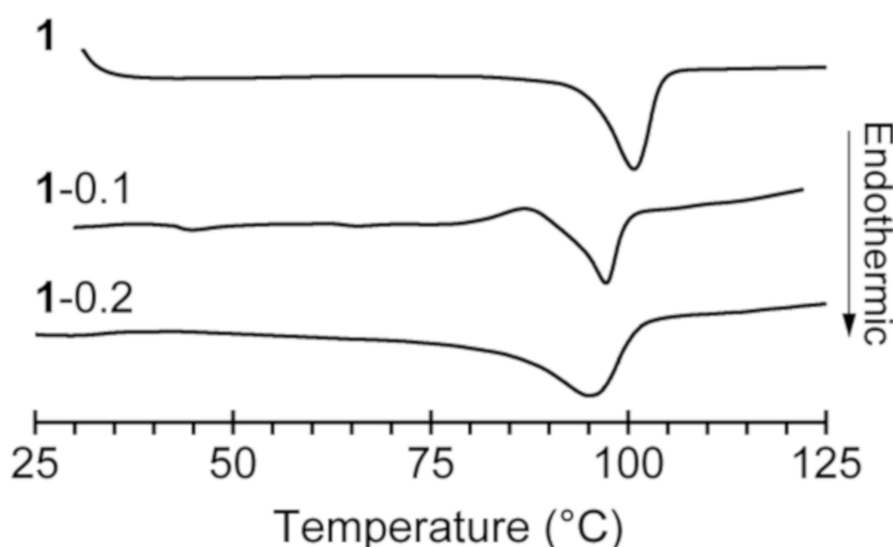


**Figure 2.** Differential scanning calorimetry (DSC) curves of **1**, **1-0.1**, and **1-0.2**.

The crystal structure of **1** was revealed by single-crystal X-ray diffractometry (XRD) at  $-120$  °C (Figure 3), which showed that the [C3mim][SCN] and  $B(C_6F_5)_3$  moieties are located in the crystal lattice of **1** in a 1:1 molar ratio. The formation of a coordinative interaction between the N atom of the thiocyanate anion and the B atom of  $B(C_6F_5)_3$  was also confirmed, since the boron center exhibits a tetrahedral structure with an average N–B–C bond angle of 107.5°. Furthermore, the B–N bond distance in **1** was determined to be 1.54 Å, while the B–N–C bond angle was found to be 165.23°. These values are comparable to those reported for compounds with B–N bonds between cyano groups and  $B(C_6F_5)_3$  [16,18]. The packing view of **1** reveals a one-dimensional arrangement of imidazolium ions and adduct-type anions along the  $b$ -axis (Figure 4).

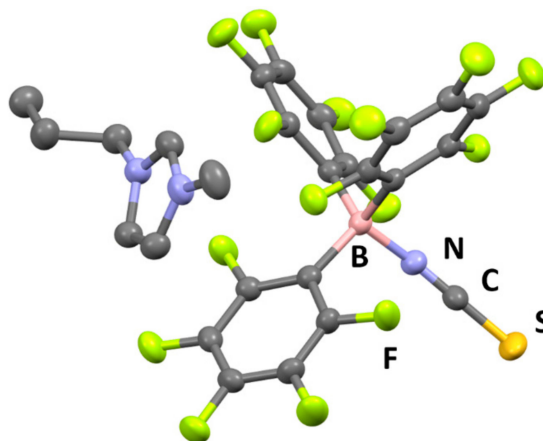


**Figure 3.** Crystal structure of **1** (C: gray, B: pink, N: blue, F: green, S: dark yellow. Thermal ellipsoids are shown at the 40% probability level. Hydrogen atoms are omitted for clarity).

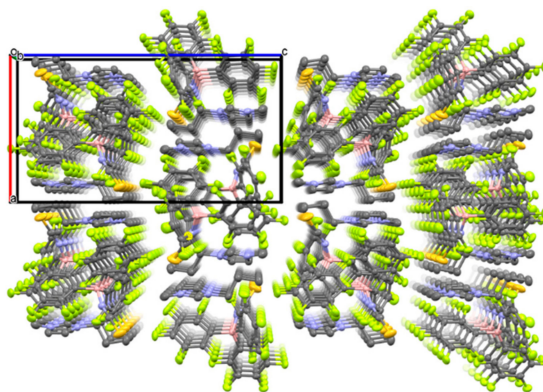


**Figure 4.** Packing view of **1** along the *b*-axis (C: gray, B: pink, N: blue, F: green, S: dark yellow. Thermal ellipsoids are shown at the 40% probability level. Hydrogen atoms are omitted for clarity).

The ion conductivity of **1** was evaluated by the ac impedance method. A disk of **1** was fabricated by grinding single crystals to a white powder followed by pressure molding; this disk was used in the conductivity experiments. Crystals of **1** exhibit a linear Arrhenius relationship between the logarithm of solid-state ion conductivity and reciprocal temperature in the 75–95 °C range (Figure 5), from which the activation energy for **1** was calculated to be 258 kJ mol<sup>-1</sup>. This value is quite large compared to those for lithium ion conduction in previously reported lithium-salt based OICs [8–11].

Based on the above result, we investigated the use of **1** as a matrix material for a solid electrolyte with sodium-ion conductivity. We expected the in situ formation of Na[SCN·BCF] when 0.1 or 0.2 molar equivalents of NaSCN and B(C<sub>6</sub>F<sub>5</sub>)<sub>3</sub> were added to **1**, these materials are referred to as “**1**-0.1” and “**1**-0.2”, respectively. DSC curves of **1**-0.1 and **1**-0.2 gave the behavior corresponding to the melting point depression in comparison with **1** (Figure 2). Solid electrolytes **1**-0.1 and **1**-0.2 were obtained by heating a solid mixture of **1** and the appropriate amounts of NaSCN and B(C<sub>6</sub>F<sub>5</sub>)<sub>3</sub> at 120 °C under argon in the absence of any solvent to give colorless viscous liquids followed by cooling to room temperature. Both **1**-0.1 and **1**-0.2 were obtained as white powders that exhibit solid-state ionic conductivity. The ionic conductivity of **1**-0.2 was determined to be 2.9 × 10<sup>-5</sup> S cm<sup>-1</sup> at 80 °C, which is 100 times higher than that of **1**.

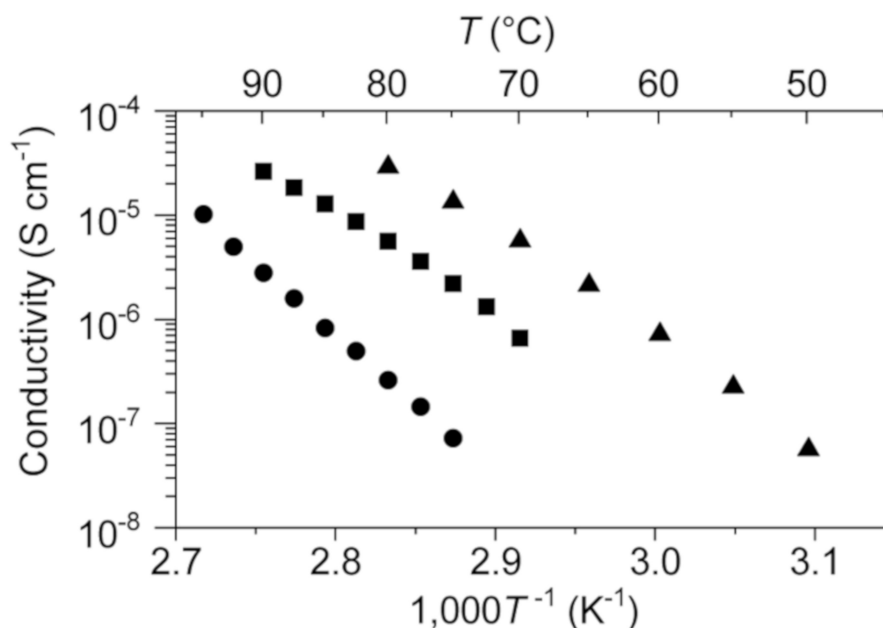


**Figure 5.** Ionic conductivities of **1** (circles), **1-0.1** (squares), and **1-0.2** (triangles) as functions of temperature.

Interestingly, the observed powder XRD patterns of **1** at room temperature were almost identical to the simulated pattern based on the crystal structure of **1** revealed by single crystal X-ray diffraction study at  $-120$  °C (Figure 6). This result shows that the crystal structure of **1** shown in Figure 3 is maintained at room temperature. Moreover, it is shown that the ordered arrangements of the imidazolium cations and the adduct-type anions in **1** depicted in Figure 4 are maintained in both **1-0.1** and **1-0.2** since the XRD patterns of **1**, **1-0.1**, and **1-0.2** are quite similar. It strongly suggests that the sodium ions in **1-0.1** and **1-0.2** occupy cationic sites or interstitial positions in the packing structure of **1**. Since the imidazolium cation and the adduct-type anion are sterically quite large compared to the sodium ion, we expect that the sodium ions diffuse through the crystal lattices of **1-0.1** and **1-0.2**.

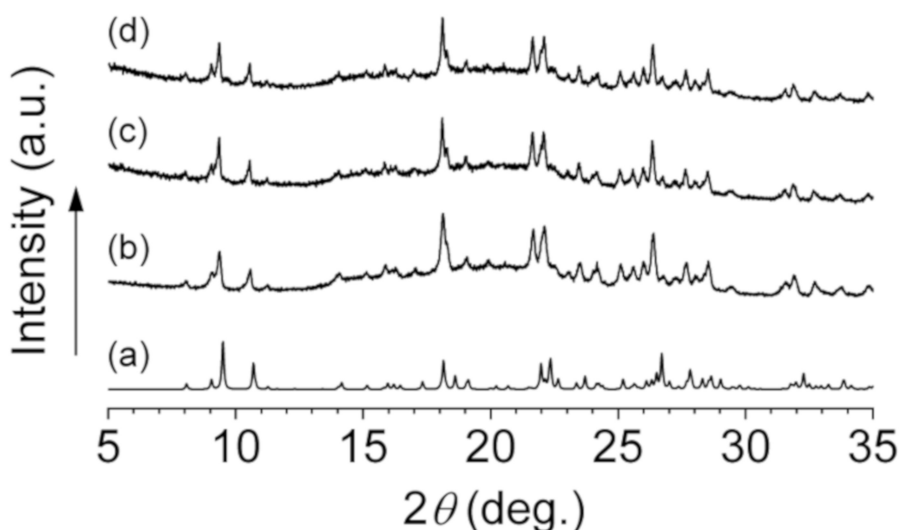


**Figure 6.** Simulated powder X-ray diffraction (XRD) pattern based on single crystal X-ray diffraction study of **1** (a), Observed powder XRD patterns of **1** (b), **1-0.1** (c), and **1-0.2** (d).

#### 4. Conclusions

We synthesized the adduct-type anion-containing OIC **1** by the addition of  $B(C_6F_5)_3$  to an SCN-anion-containing IL. Single crystal X-ray diffractometry revealed that **1** forms coordinative B–N bonds between the SCN anions and  $B(C_6F_5)_3$  moieties. We also confirmed that **1** shows solid-state ionic conductivity in the crystalline state. We also investigated doping **1** with sodium thiocyanate and  $B(C_6F_5)_3$  to evaluate the suitability of the obtained OIC as a matrix material. Both **1**–0.1 and **1**–0.2 exhibited increased ionic conductivity compared to that of **1**. These results indicate that OICs formed by the addition of bulky Lewis acids to ILs have great potential as matrix materials for the development of innovative solid electrolytes.

**Author Contributions:** M.M. conceived the concepts; Y.O. and M.M. carried out the experiment and wrote the paper.

**Funding:** This research was funded by The Iwatani Naoji Foundation and JSPS KAKENHI Grant Number 17K14460.

**Acknowledgments:** The authors acknowledge Prof. H. Suzuki, Prof. T. Takao, and Prof. M. Oishi at Tokyo Institute of Technology to carry out the elemental analysis and Kanto Denka Kogyo Co. Ltd., for generous gifts of THF complex of tris(pentafluorophenyl)borane.

**Conflicts of Interest:** The authors declare no conflict of interest. The funders had no role in the design of the study; in the collection, analyses, or interpretation of data; in the writing of the manuscript, or in the decision to publish the results.

#### References

1. Kato, T.; Yoshio, M.; Ichikawa, T.; Soberats, B.; Ohno, H.; Funahashi, M. Transport of ions and electrons in nanostructured liquid crystals. *Nat. Rev. Mater.* **2017**, *2*, 17001. [[CrossRef](#)]
2. Goossens, K.; Lava, K.; Bielawski, C.W.; Binnemans, K. Ionic Liquid Crystals: Versatile Materials. *Chem. Rev.* **2016**, *116*, 4643–4807. [[CrossRef](#)] [[PubMed](#)]
3. Kato, T. From Nanostructured Liquid Crystals to Polymer-Based Electrolytes. *Angew. Chem. Int. Ed.* **2010**, *49*, 7847–7848. [[CrossRef](#)] [[PubMed](#)]
4. Zhu, H.; MacFarlane, D.R.; Pringle, J.M.; Forsyth, M. Organic Ionic Plastic Crystals as Solid-State Electrolytes. *TRECHEM* **2019**, *1*, 126–140. [[CrossRef](#)]
5. MacFarlane, D.R.; Forsyth, M.; Howlett, P.C.; Kar, M.; Passerini, S.; Pringle, J.M.; Ohno, H.; Watanabe, M.; Yan, F.; Zheng, W.; et al. Ionic liquids and their solid-state analogues as materials for energy generation and storage. *Nat. Rev. Mater.* **2016**, *1*, 15005. [[CrossRef](#)]
6. Armel, V.; Forsyth, M.; MacFarlane, D.R.; Pringle, J.M. Organic ionic plastic crystal electrolytes; a new class of electrolyte for high efficiency solid state dye-sensitized solar cells. *Energy Environ. Sci.* **2011**, *4*, 2234–2239. [[CrossRef](#)]
7. Moriya, M. Construction of nanostructures for selective lithium ion conduction using self-assembled molecular arrays in supramolecular solids. *Sci. Technol. Adv. Mater.* **2017**, *18*, 634–643. [[CrossRef](#)] [[PubMed](#)]
8. Moriya, M.; Kato, D.; Hayakawa, Y.; Sakamoto, W.; Yogo, T. Crystal structure and solid state ionic conductivity of molecular crystal composed of lithium bis(trifluoromethanesulfonyl)amide and 1,2-dimethoxybenzene in a 1:1 molar ratio. *Solid State Ion.* **2016**, *285*, 29–32. [[CrossRef](#)]
9. Moriya, M.; Nomura, K.; Sakamoto, W.; Yogo, T. Precisely controlled supramolecular ionic conduction paths and their structure-conductivity relationships for lithium ion transport. *CrystEngComm* **2014**, *16*, 10512–10518. [[CrossRef](#)]
10. Moriya, M.; Kato, D.; Sakamoto, W.; Yogo, T. Structural design of ionic conduction paths in molecular crystals for selective and enhanced lithium ion conduction. *Chem. Eur. J.* **2013**, *19*, 13554–13560. [[CrossRef](#)] [[PubMed](#)]
11. Moriya, M.; Kitaguchi, H.; Nishibori, E.; Sawa, H.; Sakamoto, W.; Yogo, T. Molecular ionics in supramolecular assemblies with channel structures containing lithium ions. *Chem. Eur. J.* **2012**, *18*, 15305–15309. [[CrossRef](#)] [[PubMed](#)]
12. Moriya, M.; Watanabe, T.; Nabeno, S.; Sakamoto, W.; Yogo, T. Crystal structure and solid-state ionic conductivity of cyclic sulfonylamide salts with cyano-substituted quaternary ammonium cations. *Chem. Lett.* **2014**, *43*, 108–110. [[CrossRef](#)]

13. Moriya, M.; Watanabe, T.; Sakamoto, W.; Yogo, T. Combination of organic cation and cyclic sulfonylamide anion exhibiting plastic crystalline behavior in a wide temperature range. *RSC Adv.* **2012**, *2*, 8502–8507. [[CrossRef](#)]
14. LeBlanc, F.A.; Decken, A.; Cameron, T.S.; Passmore, J.; Rautiainen, J.M.; Whidden, T.K. Synthesis, Characterization, and Properties of Weakly Coordinating Anions Based on tris-Perfluoro-tert-Butoxyborane. *Inorg. Chem.* **2017**, *56*, 974–983. [[CrossRef](#)] [[PubMed](#)]
15. Fuller, A.-M.; Mountford, A.J.; Scott, M.L.; Coles, S.J.; Horton, P.N.; Hughes, D.L.; Hursthouse, M.B.; Lancaster, S.J. Synthesis, structure, and stability of adducts between phosphide and amide anions and the Lewis acids borane, tris(pentafluorophenyl)borane, and tris(pentafluorophenyl)alane. *Inorg. Chem.* **2009**, *48*, 11474–11482. [[CrossRef](#)] [[PubMed](#)]
16. Bernsdorf, A.; Brand, H.; Hellmann, R.; Köckerling, M.; Schulz, A.; Villinger, A.; Voss, K. Synthesis, structure, and bonding of weakly coordinating anions based on CN adducts. *J. Am. Chem. Soc.* **2009**, *131*, 8958–8970. [[CrossRef](#)] [[PubMed](#)]
17. Zhang, Q.; Li, M.; Zhang, X.; Wu, X. The Thermodynamic Estimation and Viscosity, Electrical Conductivity Characteristics of 1-Alkyl-3-Methylimidazolium Thiocyanate Ionic Liquids. *Z. Phys. Chem.* **2014**, *228*, 851–867. [[CrossRef](#)]
18. Jacobsen, H.; Berke, H.; Döring, S.; Kehr, G.; Erker, G.; Fröhlich, R.; Meyer, O. Lewis Acid Properties of Tris(pentafluorophenyl)borane. Structure and Bonding in L-B(C<sub>6</sub>F<sub>5</sub>)<sub>3</sub> Complexes. *Organometallics* **1999**, *18*, 1724–1735. [[CrossRef](#)]



© 2019 by the authors. Licensee MDPI, Basel, Switzerland. This article is an open access article distributed under the terms and conditions of the Creative Commons Attribution (CC BY) license (<http://creativecommons.org/licenses/by/4.0/>).